2 DOF Modelling of an aeroelastic wing

Ardrit Ramadani

Abstract

This report investigates the onset of flutter for a flat plate model of an aerofoil on a two spring system, through the use of MATLAB/SIMULINK block diagram modelling. The occurrence of flutter is predicted for a 2 DOF and 3 DOF system to occur at a standardized speed of U/b = 89, when Theodorsens functions are applied however fail to do so with a lack of them. The results produced aim to aid in the development of an active flutter reduction system for modern fly by wire aircraft.

Contents

1. Introduction

This report sets out to model the response of an aircraft wing to identify the aeroelastic effects on the structure due to the inherent elastic properties of a non-theoretical wing. A real wing is not a perfectly rigid structure and is susceptible to flexing and torsion, causing an instantaneous change in the lift and drag characteristics immediately after an external disturbance in the flow field. These are known as aeroelastic effects which are unavoidable and can cause catastrophic consequences for an aircraft if the flow velocity exceeds the maximum safe operating conditions in which the wing stiffness is able to suitably damp the oscillations produced by the disturbance.

2. Aims and Objectives

This report will produce a block diagram of the wing's response to a step disturbance through the use of MATLAB/Simulink modelled as a flat plate using the Lagrangian method and Euler-Lagrange equations including a state space representation. The flutter speed and response of the model will be investigated for the fixed flat plate in a two degree of freedom configuration as well as with a trailing flap, in a three degree of freedom configuration.

3. Background

3.1. Problem Setup

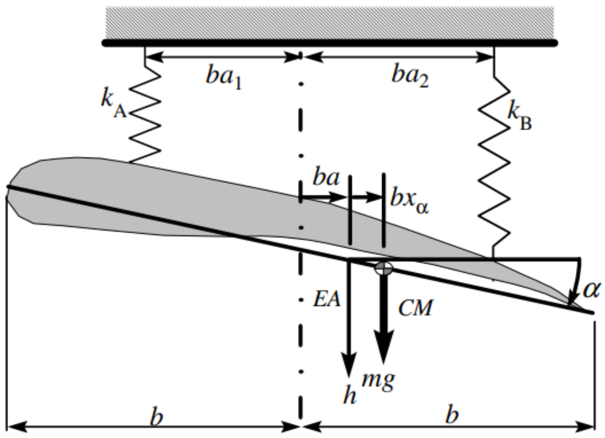

Figure 1: Setup diagram of plate representation of aerofoil

An aerofoil is represented as a flat plate of chord 2b with the weight (mg) acting at the Centre of Mass (CM), behind the point at which the coordinate system is located and sum of moments are offset, the Elastic Axis (EA). The plate is suspended on two theoretically ideal springs of stiffness k_A and k_B, allowing for two degrees of freedom in vertical (h) and angular displacement (α), about the elastic axis (Figure 1). Distances along the plate are non-dimensionalised by the semi chord length b, and the plate possesses a mass moment of inertia I_α, restoring lift (L), restoring moment (M), disturbing lift (L_G), and disturbing moment (M_G). In the case of the three degree of freedom model, a trailing edge flap is hinged at the three-quarter chord point, making a deflection angle β with the flat plate and moment M_f about the hinge point.

3.2. Methodology

The Lagrangian for the aerofoil can be calculated in terms of the Kinetic (T) and Potential (V) energies of the system in the Eularian frame for vertical and rotational components.

$$L = T - V \qquad e.q.1$$

Setting the reference frame at the elastic axis allows for the formulation of a stiffness uncoupled form of equations of motion. Taking the reference at EA, the translational and rotational kinetic energies T_1 and T_2 and the flap deflection T_3 can be represented as:

$$T_1 = \frac{1}{2}m\left(\dot{h} + bx_\alpha\dot{\alpha}\right)^2 \qquad e.q.2$$

$$T_2 = I_{cm}\dot{\alpha}^2 \qquad e.q.3$$

$$T_3 = \frac{1}{2}m_\beta\left(\left(\dot{h_\beta} + b_{x\beta}\dot{\beta}\right)^2 - \dot{h_\beta}^2\right) \qquad e.q.4$$

The summation of the above presents the total kinetic energy of the system, as;

$$T = \frac{1}{2}m\left(\dot{h} + bx_\alpha\dot{\alpha}\right)^2 + I_{cm}\dot{\alpha}^2 + \frac{1}{2}m_\beta\left(\left(\dot{h_\beta} + b_{x\beta}\dot{\beta}\right)^2 - \dot{h_\beta}^2\right) \qquad e.q.5$$

And with the potential energy due to the ideal springs being a function of their stiffness;

$$V = \frac{1}{2}k_h h^2$$

With the rotational potential energies of the plate V_r and flap V_f being;

$$V_r = \frac{1}{2}k_\alpha\alpha^2 \qquad e.q.6$$

$$V_f = \frac{1}{2}k_\beta\beta^2 \qquad e.q.7$$

The summation of which producing:

$$V = \frac{1}{2}\left(k_h h^2 + k_\alpha\alpha^2 + k_\beta\beta^2\right) \qquad e.q.8$$

Applying the Euler-Lagrange second order differential equations of;

$$\frac{d}{dt}\frac{dL}{d\dot{q}} - \frac{dL}{dq} = 0 \qquad e.q.9$$

Leads to the simplified equations of motion excluding the aerodynamic effects;

$$m\ddot{h} + mbx_\alpha\ddot{\alpha} + k_h h = 0 \qquad e.q.10$$

$$mbx_\alpha\ddot{h} + I_\alpha\ddot{\alpha} + k_\alpha h = 0 \qquad e.q.11$$

In which including the aforementioned aerodynamic effects of lift, moment and their disturbing forces leads to;

$$m\ddot{h} + mbx_\alpha\ddot{\alpha} + k_h h + L = L_G \qquad e.q.12$$

$$mbx_\alpha\ddot{h} + I_\alpha\ddot{\alpha} + k_\alpha h + M = M_G \qquad e.q.13$$

With the third order state space formulation being in the form;

$$A\ddot{x} + B\dot{x} + Cx + D\,, x = [h \quad \alpha]^T$$

Giving;

$$\begin{bmatrix} L \\ M \end{bmatrix} = M_a \begin{bmatrix} \ddot{h} \\ \ddot{\alpha} \end{bmatrix} + C_a \begin{bmatrix} \dot{h} \\ \dot{\alpha} \end{bmatrix} + K_a \begin{bmatrix} h \\ \alpha \end{bmatrix} \qquad e.q.14$$

Where;

$$M_a = \pi\rho b^3 \begin{bmatrix} \frac{1}{b} & -a \\ -a & b\left(a^2 + \frac{1}{8}\right) \end{bmatrix}$$

$$C_a = \pi\rho b^2 U \begin{bmatrix} \frac{2C(k)}{b} & 1 + C(k)(1-2a) \\ -C(k)(1+2a) & b\left(\frac{1}{2} - a\right)\left(1 - C(k).(1+2a)\right) \end{bmatrix}$$

$$K_a = \pi\rho b U^2 C(k) \begin{bmatrix} 0 & 2 \\ 0 & -b(1+2a) \end{bmatrix}$$

In which the inclusion of a flap produces;

$$\begin{bmatrix} mb^2 & mb^2x_\alpha & m_\beta b^2 x_\beta \\ mb^2x_\alpha & I_\alpha & m_\beta b^2 x_\beta(c-a) + I_\beta \\ m_\beta b^2 x_\beta & m_\beta b^2 x_\beta(c-a) + I_\beta & I_\beta \end{bmatrix} \begin{bmatrix} \frac{\ddot{h}}{b} \\ \ddot{\alpha} \\ \ddot{\beta} \end{bmatrix} + \begin{bmatrix} k_h b^2 & 0 & 0 \\ 0 & k_\alpha & 0 \\ 0 & 0 & k_\beta \end{bmatrix} \begin{bmatrix} \frac{h}{b} \\ \alpha \\ \beta \end{bmatrix} + \begin{bmatrix} Lb \\ -M \\ -M_\beta \end{bmatrix} = \begin{bmatrix} 0 \\ 0 \\ 0 \end{bmatrix} e.q.15$$

Where;

$$\begin{bmatrix} Lb \\ -M \\ -M_\beta \end{bmatrix} = \pi\rho b^2 U^2 \left(\widetilde{M}_a \begin{bmatrix} \frac{\ddot{h}}{b} \\ \ddot{\alpha} \\ \ddot{\beta} \end{bmatrix} + \tilde{C}_a \begin{bmatrix} \frac{\dot{h}}{b} \\ \dot{\alpha} \\ \dot{\beta} \end{bmatrix} + \widetilde{K}_a \begin{bmatrix} \frac{h}{b} \\ \alpha \\ \beta \end{bmatrix} \right)$$

With the Matrices defined as;

$$\widetilde{M}_a = \left(\frac{b}{U}\right)^2 \begin{bmatrix} 1 & -a & -\frac{T_1}{\pi} \\ -a & \left(a^2 + \frac{1}{8}\right) & 2\frac{T_{13}}{\pi} \\ -\frac{T_1}{\pi} & 2\frac{T_{13}}{\pi} & \frac{T_3}{\pi^2} \end{bmatrix} \qquad e.q.16$$

$$\tilde{C}_a = \tilde{C}_{anc} + \tilde{C}_{ac-ntl} + \tilde{C}_{ac-tl}C(k) \qquad e.q.17$$

$$\tilde{C}_{anc} = \frac{b}{U}\begin{bmatrix} 0 & 1 & -\frac{T_4}{\pi} \\ -1 & 0 & \frac{T_{15}}{\pi} \\ \frac{T_4}{\pi} & \frac{T_{15}}{\pi} & 0 \end{bmatrix} \qquad e.q.18$$

$$\tilde{C}_{ac-ntl} = \frac{b}{U}\begin{bmatrix} 0 \\ 1 \\ -\frac{T_4}{\pi} \end{bmatrix}\begin{bmatrix} 1 & \left(\frac{1}{2} - a\right) & \frac{T_{11}}{\pi} \end{bmatrix} \qquad e.q.19$$

$$\tilde{C}_{ac-tl} = \frac{b}{U}\begin{bmatrix} 2 \\ -(1+2a) \\ \frac{T_{12}}{\pi} \end{bmatrix}\begin{bmatrix} 1 & \left(\frac{1}{2} - a\right) & \frac{T_{11}}{\pi} \end{bmatrix} \qquad e.q.20$$

$$\widetilde{K}_a = \widetilde{K}_{anc} + \widetilde{K}_{ac-ntl} + \widetilde{K}_{ac-tl}C(k) \qquad e.q.21$$

$$\widetilde{K}_a = \begin{bmatrix} 0 & 0 & 0 \\ 0 & -1 & \frac{T_4}{\pi} \\ 0 & \frac{T_4}{\pi} & \frac{T_5}{\pi^2} \end{bmatrix} \qquad e.q.22$$

$$\widetilde{K}_{ac-ntl} = \begin{bmatrix} 0 \\ 1 \\ -\frac{T_4}{\pi} \end{bmatrix}\begin{bmatrix} 0 & 1 & \frac{T_{10}}{\pi} \end{bmatrix} \qquad e.q.23$$

$$\widetilde{K}_{ac-tl} = 2\begin{bmatrix} 1 \\ -\left(\frac{1}{2} + a\right) \\ \frac{T_{12}}{2\pi} \end{bmatrix}\begin{bmatrix} 0 & 1 & \frac{T_{10}}{\pi} \end{bmatrix} \qquad e.q.24$$

With the linear representation as;

$$\left(M + Sq\widetilde{M}\right)\ddot{x} + \left(C + Sq\widetilde{M}\right)\dot{x} + \left(K + Sq\widetilde{M}\right)x = -\begin{bmatrix} \bar{L}_G & \bar{M}_G & \bar{M}_{\beta G} \end{bmatrix}^T \qquad e.q.25$$

Where

$$S = 2\pi b^2, q = \frac{1}{2}\rho U^2, x = \begin{bmatrix} \frac{h}{b} & \alpha & \beta \end{bmatrix}^T$$

In the above the variable of C(k) is that from the Theodorsens functions where;

$$C(k) = 1 - \frac{0.165(ik)}{ik + 0.0455} - \frac{0.335(ik)}{ik + 0.3} \qquad e.q.26$$

From values within the Theodorsens function table, Appendix A, of which the Laplacian transform can be applied to provide a transferred function of (s);

$$T(s) = 1 - \frac{0.165s}{s + \frac{0.0455}{b}} - \frac{0.335s}{s + \frac{0.3}{b}} \qquad e.q.27$$

4. Procedure

4.1. 2 Degrees of Freedom

The model will begin with a two degree of freedom model for the equations of motion.

$$\begin{bmatrix} \bar{L}_G b \\ \bar{M}_G \end{bmatrix} = \begin{bmatrix} 1 & x_a \\ x_a & I_a/_{mb^2} \end{bmatrix} \begin{bmatrix} \frac{\ddot{h}}{b} \\ \ddot{\alpha} \end{bmatrix} + \begin{matrix} \frac{k_h}{m} & 0 \\ 0 & \frac{k_\alpha}{mb^2} \end{matrix} \begin{bmatrix} \frac{\dot{h}}{b} \\ \dot{\alpha} \end{bmatrix} + \begin{bmatrix} \frac{h}{b} \\ \alpha \end{bmatrix} \qquad e.q.28$$

$$\begin{bmatrix} \bar{L}b \\ \bar{M} \end{bmatrix} = \frac{\pi \rho b^2}{m} \left(\tilde{M}_a \begin{bmatrix} \frac{\ddot{h}}{b} \\ \dot{\alpha} \end{bmatrix} + \tilde{C}_{a-nc} \begin{bmatrix} \frac{\ddot{h}}{b} \\ \dot{\alpha} \end{bmatrix} \right) \qquad e.q.29$$

With the highest order from e.q.15 made the subject, and reduced by mb^2, in order to produce a state space model suitable for an iterative solution, giving the final representation for the two degree of freedom with no Theodorsen function as;

$$\begin{bmatrix} \ddot{h}/_b \\ \ddot{a} \end{bmatrix} = \begin{bmatrix} 1 & x_a \\ x_a & I_a/_{mb^2} \end{bmatrix}^{-1} \left(\begin{bmatrix} \bar{L}_G b \\ \bar{M}_G \end{bmatrix} - \begin{bmatrix} k_h/_m & 0 \\ 0 & k_a/_{mb^2} \end{bmatrix} \begin{bmatrix} h/_b \\ \alpha \end{bmatrix} \right) \qquad e.q.30$$

In which the Theodorsen can be applied, giving;

$$\begin{bmatrix} \tilde{L}_c b \\ \tilde{M}_c \end{bmatrix} = 2 \begin{bmatrix} 1 \\ -\left(\frac{1}{2} + a\right) \end{bmatrix} C(k) \left(\frac{U}{b} \begin{bmatrix} 1 & \left(\frac{1}{2} - a\right) \end{bmatrix} \frac{d}{dt} \begin{bmatrix} \frac{h}{b} \\ \alpha \end{bmatrix} + \left(\frac{U}{b}\right)^2 \begin{bmatrix} 0 & 1 \end{bmatrix} \begin{bmatrix} \frac{h}{b} \\ \alpha \end{bmatrix} \right) \qquad e.q.31$$

Where the C(k) value and transferred function can be found from e.q.26 & 27 respectively.

Table 1: 2 DOF parameters

Parameter	Equation
R	$r_a^2 + \frac{a^2}{\mu} + \frac{1}{8\mu}$
S	$x_a - \frac{a}{\mu}$
K	ω_h^2
P	$r_\alpha^2 \omega_\alpha^2$
$\bar{U}$	$\frac{U}{b}$
μ	$\frac{m}{\pi \rho b^2}$

Table 2: Derivative values

Parameter	x_a	$r_a^2 = \frac{I_a}{mb^2}$	$\omega_{h0}^2 = \frac{k_h}{m}$	$\omega_{a0}^2 = \frac{k_a}{I_a}$	μ
Value	0.2	0.25	3300	10000	10

4.2. 3 Degree of freedom model

The three degree of freedom matrix found in e.q.15 is to represented as a single function in the form of

$$M_s\ddot{x} + K_s x + L = 0 \qquad e.q.32$$

Giving

$$(M_s + \pi\rho b^3 U^2 \widetilde{\boldsymbol{M}}_{\boldsymbol{a}})\ddot{\boldsymbol{x}} + \pi\rho b^3 U^2 (\widetilde{\boldsymbol{C}}_{\boldsymbol{ac-tl}} + \widetilde{\boldsymbol{C}}_{\boldsymbol{ac-ntl}})\dot{\boldsymbol{x}} + K_s x + \pi\rho b^3 U^2 (\widetilde{\boldsymbol{K}}_{\boldsymbol{anc}} + \widetilde{\boldsymbol{K}}_{\boldsymbol{ac-ntl}})x + \pi\rho b^3 U^2 \big(C(k)(\widetilde{\boldsymbol{C}}_{\boldsymbol{ac-tl}} + \widetilde{\boldsymbol{K}}_{\boldsymbol{ac-tl}})\big) = 0$$

5. Block Diagram

5.1. Two Degrees of Freedom with no Theodorsens functions

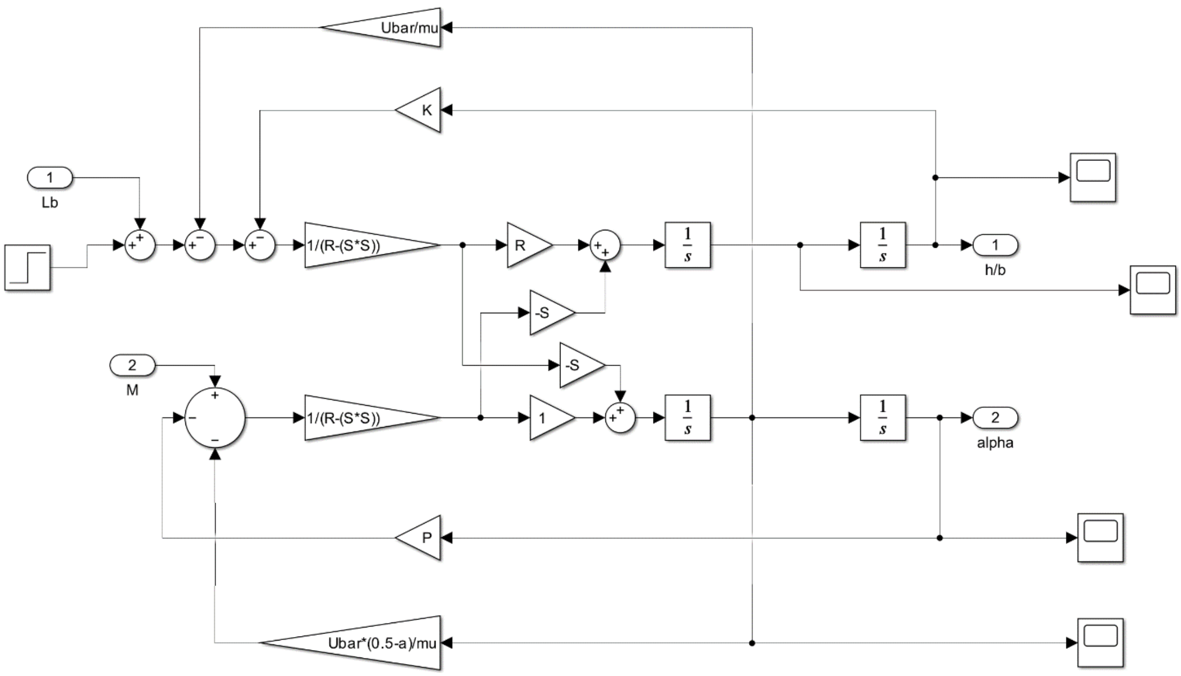

5.2. Two Degrees of Freedom With Theodorsens functions

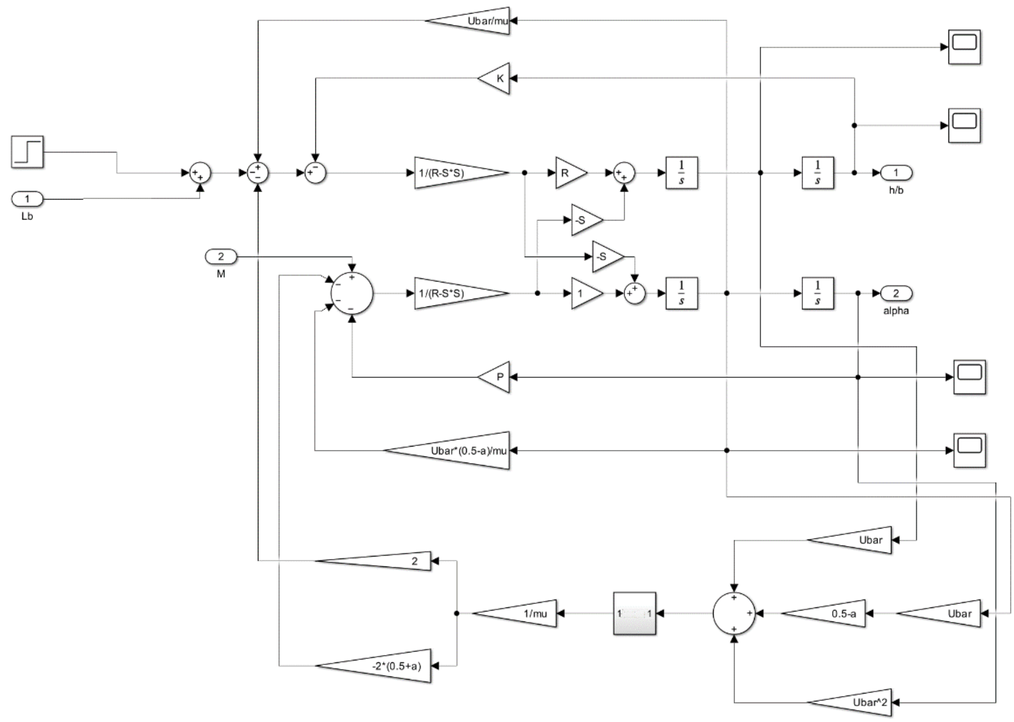

5.3. Three Degrees of Freedom with Theodorsens functions

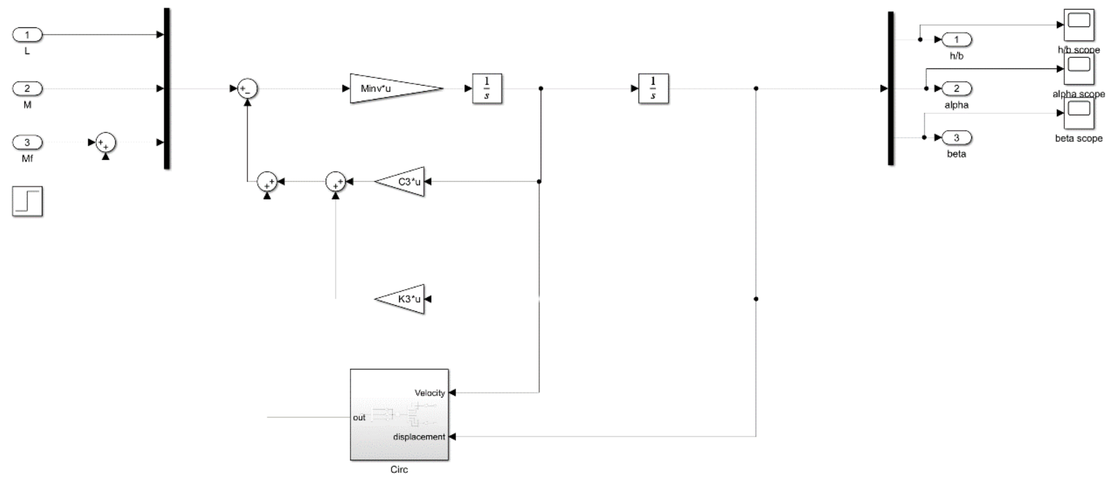

5.4. Three DOF subroutine

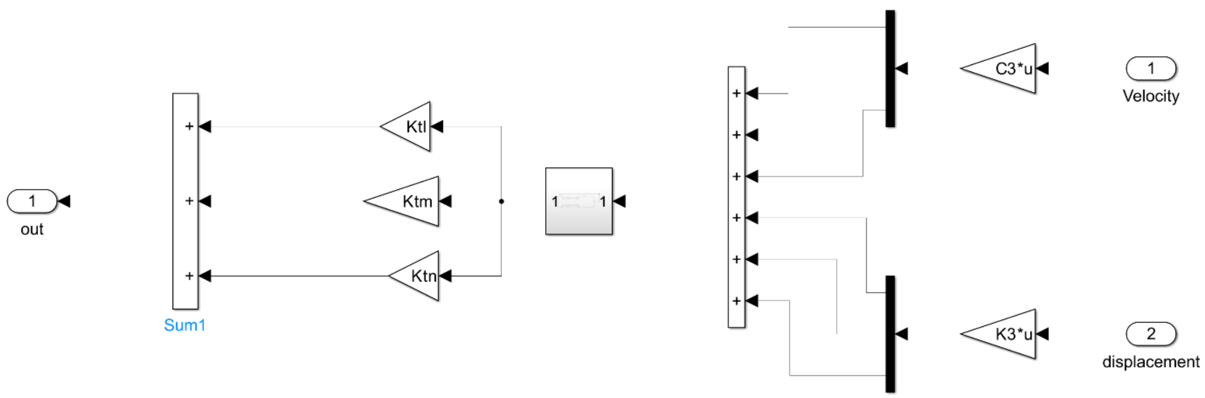

5.5. Transfer function, C(k)

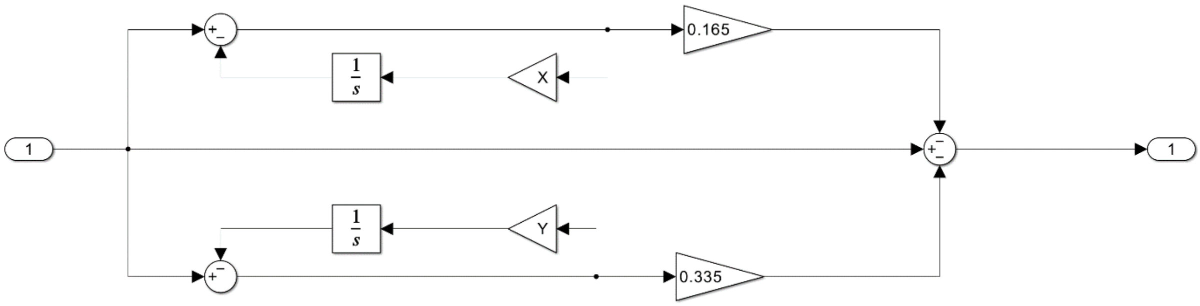

6. Results

6.1. Two degrees of freedom with no Theodorsens functions

	$\bar{U} = 10$	$\bar{U} = 100$	$\bar{U} = 200$
$\frac{h}{b}$	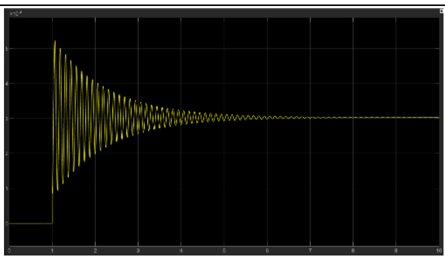	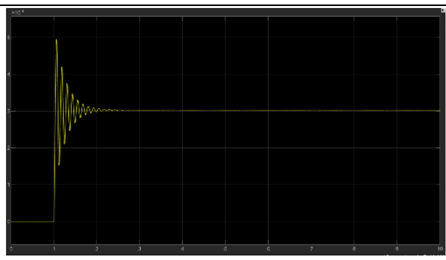	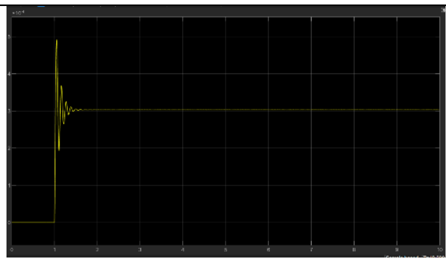
α	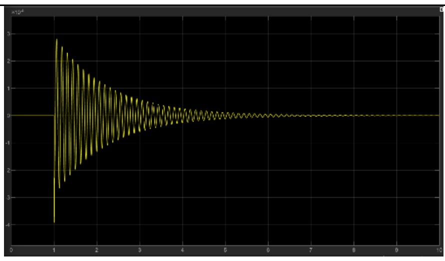	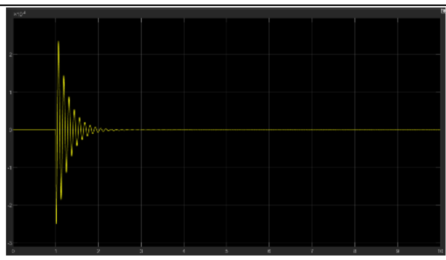	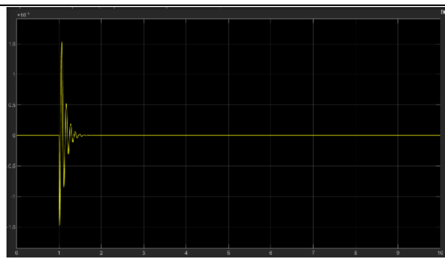

Figure 2 Transient values of h/b and alpha for 2 DOF with no Theodorsens for U = 10,100,200

6.2. With Theodorsens functions

	$\bar{U} = 10$	$\bar{U} = 100$
$\frac{h}{b}$	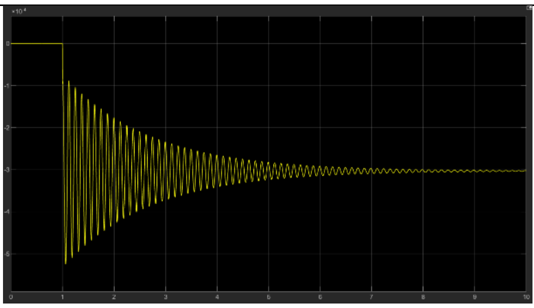	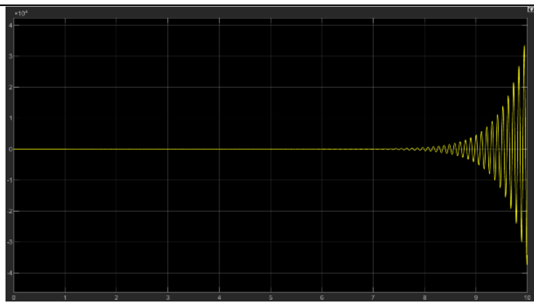
α	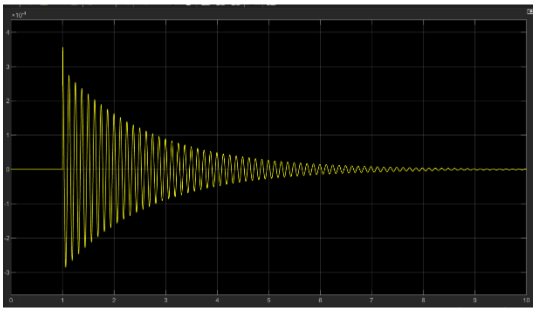	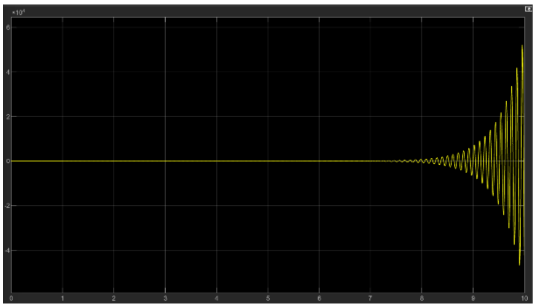

Figure 3:Transient values of h/b and alpha for 2 DOF with Theodorsens for U = 10,100

	$\bar{U} = 88$	$\bar{U} = 89$	$\bar{U} = 90$
$\frac{h}{b}$	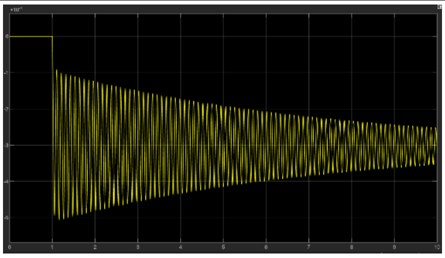	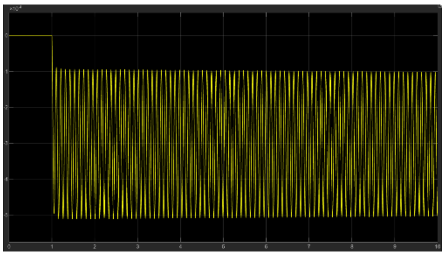	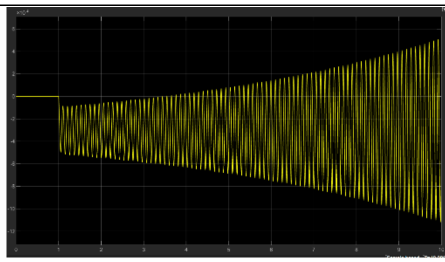
α	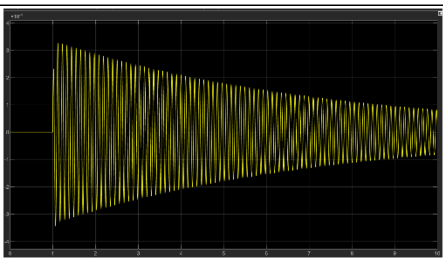	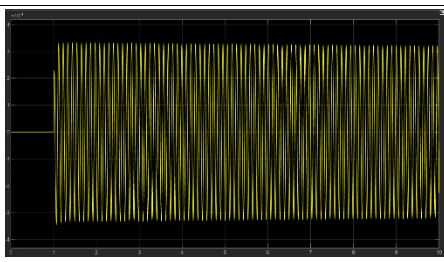	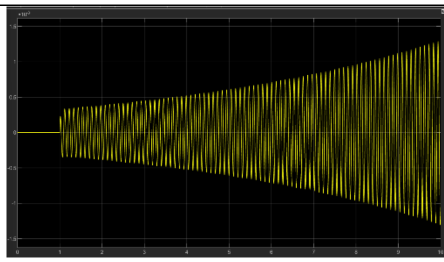

Figure 4:Transient values of h/b and alpha for 2 DOF with Theodorsens for U close to flutter

6.3. 3DOF

	$\bar{U} = 10$	$\bar{U} = 100$
$\frac{h}{b}$	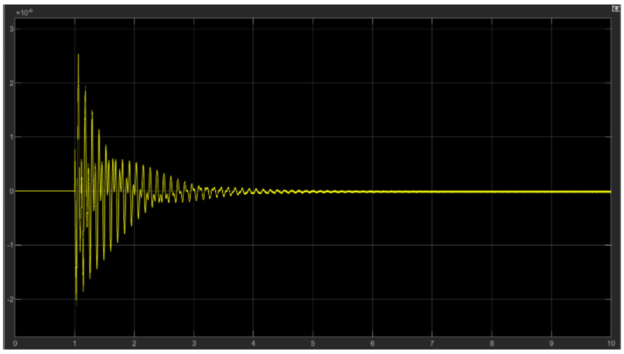	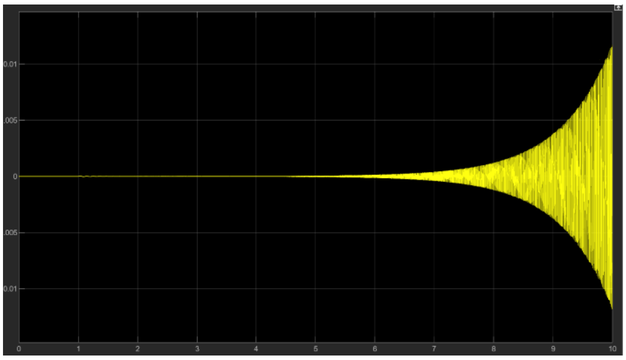
α	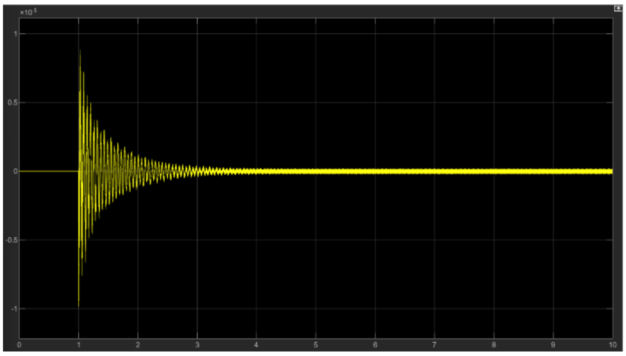	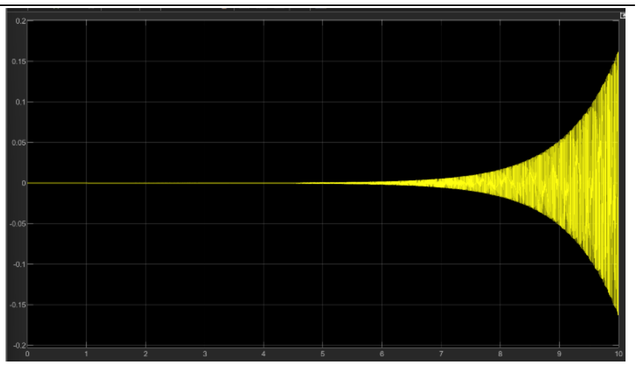
β	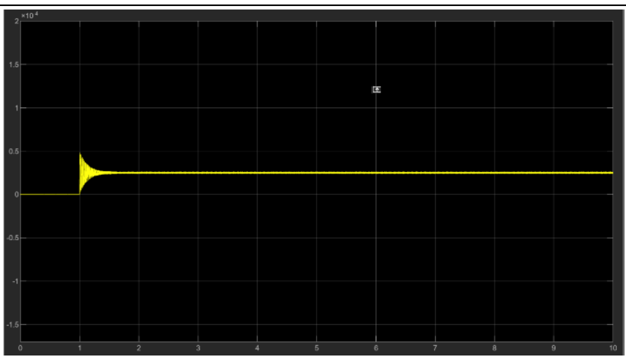	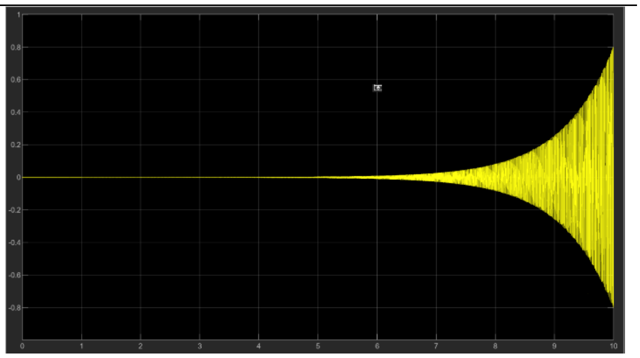

Figure 5:Transient values of h/b, alpha and beta for 3 DOF with Theodorsens for U = 10,100

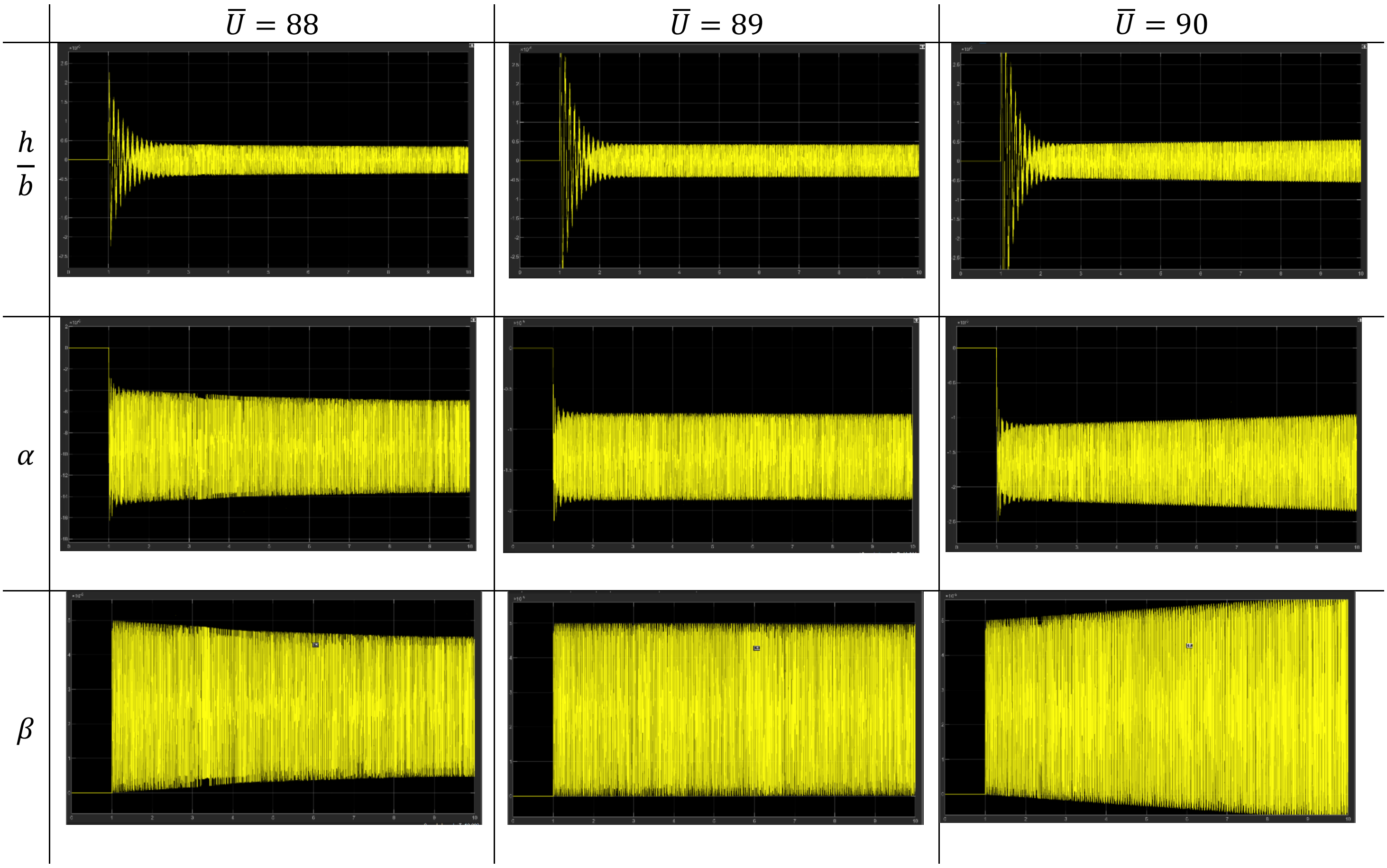

Figure 6:Transient values of h/b, alpha and beta for 3 DOF with Theodorsens for U close to flutter

7. Discussion

The aeroelastic characteristic of a flat plate in the representation of an aerofoil has been shown to be able to be modelled through the Euler-Lagrange formulation and Theodorsen functions. This was possible for the 2DOF and 3DOF models with Theodorsen functions but was not achieved for the model lacking the function. The two degree of freedom model without the use of the Theodorsen function in Figure 2 showed a translational and angular displacement which became more stable as the relative speed was increased, never reaching a flutter point within the scope of the analysis. This contradicts modern theory and suggests that either the method of modelling is not adequate or that significant numerical error had been encountered through the integrating processes leading to a large artificial damping effect.

The models including Theodorsens function on the other hand proved successful and agreed with modern literature, finding that a critical flow speed will induce a flutter oscillation which can cause a catastrophic event (Chai Y et al, 2021). The modelling not including a trailing flap Figure 4 showed a constant reduction in the inertial damping effect, causing oscillations to take an increasing time to dissipate with an increase in flow velocity. This increased to the point where flutter was observed at a standardized velocity of U/b = 89, after which the translation and pitch angle rapidly diverged causing instability due to a perturbation in flow field.

The three degree of freedom model showed similarly to the two degree of freedom model that a flutter speed for the model could be predicted at similar values by both methods. The model with a trailing edge flap also showed a flutter speed just above U/b = 89, Figure 6, with a higher frequency of oscillations. The overall stability response with a trailing flap was reduced as compared to an entirely flat plate, showing less damping, with the flap angle having rapid oscillations of a higher magnitude. The results presented have been in agreement across the 2DOF and 3DOF models with good confidence however are assumed on the theoretically ideal formation of the model with ideal springs and no wear due to excessive use or cyclic loading being accounted for. In a real flight scenario, the wing is likely to undergo many loading cycles which can reduce the inertial and stiffness damping effects and lead to a more brittle wing, causing the critical velocity to induce flutter to be reduced. Additionally, within the theoretical modelling the changes in the centre of gravity, centre of pressure and position of the elastic axis during flight and operation of the trailing edge flap, while small, will be exacerbated during higher acceleration manoeuvres, adding further inaccuracy to the model.

The model has however shown the ability for a computationally efficient method of predicting the deflections in displacement, angle and flap angle as well as the onset of flutter and the critical speed at which it would theoretically occur, with potential modifications it could prove useful in the digital twin age in the implementation of an active flutter suppression system.

Given an adequate fly by wire system, the model could be implemented into a larger scale active suppression system using a closed loop state space controller. An active system primarily uses a closed loop control system in which the states of the wing are monitored and actuations in the flap angle or alternate control surface, such as piezoelectric layers suggested by (Chai Y et al, 2021), to control the effective angle of attack of the wing or manipulate the flow over the wing.

The successful implementation of the 3DOF model could be carried out assuming a suitable sensor array could be sourced to act as the observers for the model, including several 6 axis INS, measuring the inertial movements of the aircraft and wing tips individually, which would be able to provide real time feedback to a series of actuators along the trailing flap to continuously alter the deflection angle.

In addition to the technical systems required, in flight testing as outlined by (Kayran, A) could be carried out to verify the inertial and mass/ aerodynamic matrices in order to increase the accuracy of the model for a larger flight envelope as well as outlining a suitable safety margin in which precautionary measures could be taken by the system to reduce the overall flight speed if the onset of flutter is detected.

8. Conclusion

The modelling of an aerofoil as a flat plate suspended under the influence of two theoretically ideal springs was carried out in the configurations of a 2 degree of freedom model, both with and without the implementation of the Theodorsen functions, and in a three dree of freedom model with a trailing edge flap. The modelling without the Theodorsens functions proved inconclusive and were unable to predict flutter on the described setup, requiring more analysis of the points of failure of the system. The 2 degree and 3 degree of freedom models with Theodorsens functions were both able to model the flutter phenomena and produced results in agreement with each other for their respective cases finding that a normalised flutter speed U/b = 89 was present for both models. Perturbations encountered at a higher velocity would cause oscillatory fluctuations at the resonant frequency and lead to a catastrophic failure of the wing.
The report also discussed the necessity for a set of observers and actuators in order to form a full closed loop feedback system in the implementation of an active flutter suppression system for a modern fly by wire aircraft.

9. References

Chai Y, Gao W, Ankay B, Li F, Zhang C. Aeroelastic analysis and flutter control of wings and panels: A review. Int J Mech Syst Dyn. 2021; 1: 5-34.doi:10.1002/msd2.12015

Kayran, A. (2007), "Flight flutter testing and aeroelastic stability of aircraft", Aircraft Engineering and Aerospace Technology, Vol. 79 No. 2, pp. 150-162. https://doi.org/10.1108/00022660710732707

Appendix A: Table of Theodorsen's *T*-functions, T_i, i =1, 2, 3..., $\phi_c = \cos^{-1} c$, c = distance of the control surface hinge line from mid-chord in semi-chords, a = distance of the elastic axis from mid-chord in semi-chords.

I	$T_i = T_i(c,a),\ \phi_c = \cos^{-1} c.\ p \equiv -\frac{1}{3}\left(\sqrt{1-c^2}\right)^3$
1	$-\frac{1}{3}\sqrt{1-c^2}\left(2+c^2\right)+c\phi_c = 2p - cT_4$
2	$c\left(1-c^2\right)-\sqrt{1-c^2}\left(1+c^2\right)\phi_c + c\phi_c^2 = T_6$
3	$-\frac{1}{8}\left(4+5c^2\right)\left(1-c^2\right)+\frac{1}{4}c\left(7+2c^2\right)\sqrt{1-c^2}\,\phi_c - \frac{1}{8}\left(1+8c^2\right)\phi_c^2$
4	$c\sqrt{1-c^2}-\phi_c$
5	$-\left(1-c^2\right)+2c\sqrt{1-c^2}\,\phi_c - \phi_c^2$
6	$c\left(1-c^2\right)-\sqrt{1-c^2}\left(1+c^2\right)\phi_c + c\phi_c^2 = T_2$
7	$-\frac{1}{8}\left(1+8c^2\right)\phi_c + \frac{1}{8}c\left(7+2c^2\right)\sqrt{1-c^2} = \frac{1}{8}\left(1+8c^2\right)T_4 + \frac{6}{8}c\left(\sqrt{1-c^2}\right)^3$
8	$c\phi_c - \frac{1}{3}\left(1+2c^2\right)\sqrt{1-c^2} = p - cT_4,\ \left(p = T_8 + cT_4\right),$
9	$\frac{1}{6}\left(\sqrt{1-c^2}\right)^3 + \frac{a}{2}\left(c\sqrt{1-c^2}-\phi_c\right) \equiv \frac{1}{2}\left(-p + aT_4\right),$
10	$\sqrt{1-c^2}+\phi_c = -T_4 + \left(1+c\right)\sqrt{1-c^2}$
11	$\sqrt{1-c^2}\left(2-c\right)+\phi_c\left(1-2c\right) = 2T_{10}\left(1-c\right)+T_4$
12	$\sqrt{1-c^2}\left(2+c\right)-\phi_c\left(1+2c\right) = 2T_{10}\left(1-c\right)+3T_4$
13	$-\frac{1}{2}\left(T_7 + \left(c-a\right)T_1\right)$
14	$\frac{1}{16}+\frac{1}{2}ac$
15[3]	$T_1 - T_8 - \left(c-a\right)T_4 = p - \left(c-a\right)T_4 = T_1 + 2T_9$
20	$-\sqrt{1-c^2}+\phi_c$
21	$\sqrt{\left(1+c\right)/\left(1-c\right)}$
23	$\left(2\left(a-c\right)-1\right)\sqrt{1-c^2}$
24	$T_8 + \left(c-a\right)T_4 = -2T_9$

Appendix B: M file for the initialisation of values for MATLAB/Simulink models

```
Ubar = %Variable
mu = 10;
a = -0.4;
c=0.5;
mb=0.2;
ra2 = 0.25;
rb2 = 0.03;
xa = 0.2;
xb = 0.15;
R = (0.25^2) + ((-0.4^2)/10) + (1/(8*10));
S = 0.2 - ( -0.4/10);
K = 3300;
P = 0.25^2 * 10000;
X = 0.455*Ubar;
Y = 0.3*Ubar;
cc=cos(c)^-1;
sc= sqrt(1-(c^2));
c2=1-(c^2);
p=-(1/3)*(sc^3);
T1=-(1/3)*sc*(2+c^2)+(c*cc);
T3=-((1/8)*((4+(5*c^2)))*sc)+((1/4)*c*(7+(2*c^2))*cc*sc)-(1/8)*(1+(8*c^2))*(cc^2);
T4=c*sc-cc; T5 = 2*c*sc*cc-sc-(cc^2);
T7=(1/8)*c*(1+8*c^2)*T4+(6/8)*c*(sc^3);
T8 = p-c*T4;
T9=(1/2)*(-p)+a*T4; T10 =sc+cc;
T11=2*(T10)*(1-c)+T4;
T12=2*(T10)*(1-c)+3*T4;
T13=-(1/2)*(T7+(c-a)*T1);
T14=(1/16)+(1/2)*a*c;
T15=T1-T8-(c-a)*T4;
T20=-sc+cc;
T21=sqrt((1+c)/(1-c));
T23=(2*(a-c)-1)*(sqrt(1)-c^2);
T24=-2*T9;
Ms=[1 xa (mb)*xb; xa ra2 (mb)*xb*(c-a)+rb2; (mb)*xb (mb)*xb*(c-a)+rb2 rb2];
Ma = (1/mu)*[1 -a (-T1/pi); -a (a^2 + 1/8) 2*(T13/pi); (-T1/pi) 2*(T13/pi) -T3/(pi^2)];
M= (Ms + Ma);
Minv = inv(M) ;
Canc = [0 1 (-T4/pi); -1 0 (T15/pi); (T4/pi) (-T15/pi) 0];
Cacntl = [0; 1; -T4/pi]*[1 (0.5-a) T11/(2*pi)];
Ks = [K 0 0; 0 P 0; 0 0 Q];
C3 = (1/mu) *Ubar * (Canc + Cacntl);
Kanc = [0 0 0; 0 -1 T4/pi; 0 T4/pi T5/(pi^2)];
Kacntl = [0; 1; -T4/pi]*[0 1 T10/pi];
K3 = Ks + (Ubar^2)/mu * (Kanc + Kacntl) ;
CCk = (1/mu)*Ubar* [1 (0.5-a) (T11/(2*pi) )];
KCk = ((Ubar^2)/mu)*[0 1 T10/pi];
Ktm = - (1+2*a);
Ktn = T12/pi;
Ktl = 2;
C2 = Ubar^-1*[2;-(1+2*a);(T12/pi)]*[1 ((1/2)-a) (T11/pi)];
K2 = 2*[1;-((1/2)+a);(T12/2*pi)]*[0 1 (T10/pi)];
```